

# Quantum Dots in Strong Magnetic Fields: Stability Criteria for the Maximum Density Droplet\*

A. H. MacDonald,<sup>A</sup> S. R. Eric Yang<sup>A,B</sup> and M. D. Johnson<sup>C</sup>

<sup>A</sup> Department of Physics, Indiana University,  
Bloomington, IN 47405, U.S.A.

<sup>B</sup> Permanent address: IMS, NRC of Canada,  
Ottawa K1A 0R6, Canada.

<sup>C</sup> Department of Physics, University of Central Florida,  
Orlando, FL 32816-2385, U.S.A.

## Abstract

In this article we discuss the ground state of a parabolically confined quantum dot in the limit of very strong magnetic fields where the electron system is completely spin-polarised and all electrons are in the lowest Landau level. Without electron–electron interactions the ground state is a single Slater determinant corresponding to a droplet centred on the minimum of the confinement potential and occupying the minimum area allowed by the Pauli exclusion principle. Electron–electron interactions favour droplets of larger area. We derive *exact* criteria for the stability of the maximum density droplet against edge excitations and against the introduction of holes in the interior of the droplet. The possibility of obtaining exact results in the strong magnetic field case is related to important simplifications associated with broken time-reversal symmetry in a strong magnetic field.

## 1. Introduction

Advances in nanofabrication technology have made it possible to realise artificial systems in which electrons are confined to a small area within a two-dimensional electron gas. There has been considerable interest in the physics of electron–electron and electron–hole interactions in these ‘quantum dot’ systems (see e.g. Merkt 1990; Chakraborty 1992; Kastner 1992). Recent experiments have demonstrated the possibility of probing their properties in the regimes of the integer (see e.g. McEuen *et al.* 1991, 1992) and fractional (see e.g. Hansen *et al.* 1989) quantum Hall effects (see e.g. von Klitzing *et al.* 1980; Tsui *et al.* 1982). Excited states and low-temperature thermodynamic properties of quantum dots coupled to particle reservoirs are discussed elsewhere (see e.g. MacDonald and Johnson 1992). We focus here on the stability of the maximum-density-droplet (MDD) state which is the ground state in the absence of electron–electron interactions. One interesting consequence of the strong magnetic fields is that this state remains an *exact* eigenstate of the many-particle Hamiltonian even in the presence of electron–electron interactions. In Section 2 of this paper we discuss the MDD state. We point out that finite-size effects on the dependence

\* Paper presented at the Gordon Godfrey Workshop, University of New South Wales, Sydney, 20–21 July 1992.

of the MDD state energy on particle number are dominated by one-body terms from the confinement potential, rather than by the Coulomb interactions, as is usually assumed. In Section 3 we discuss the low-lying edge excitations of the MDD state and derive a criterion for the stability of the dot against edge excitations. In Section 4 we consider the introduction of holes near the centre of the MDD. We find that because of the qualitative differences which exist between two- and three-dimensional electrostatics the MDD becomes unstable against these excitations before the edge becomes unstable. Some concluding remarks are contained in Section 5.

## 2. The Maximum Density Droplet

We consider a system of electrons confined to a finite area of a two-dimensional electron gas by a parabolic potential,  $V(r) = 1/2m\Omega^2r^2$ . In the strong magnetic field limit, where  $\Omega/\omega_c \ll 1$ , only the states in the lowest Landau level are relevant. (Here  $\omega_c = eB/mc$  is the cyclotron frequency.) In the symmetric gauge the single-particle states  $[\phi_l(z) \sim z^l \exp(-z\bar{z}/4\ell^2)]$  in this level may be labelled by angular momentum and have energy (see e.g. Merkt 1990; Chakraborty 1992; Kastner, 1992)  $\varepsilon_l = \hbar\omega_c/2 + \gamma(l+1)$ , where  $\gamma = m\Omega^2\ell^2 = \hbar\omega_c(\Omega/\omega_c)^2$ . [Here  $z = x + iy$  is the 2D electron coordinate expressed as a complex number,  $\ell \equiv (\hbar c/eB)^{1/2}$  is the magnetic length, and the allowed values of single-particle angular momentum within the lowest Landau level are  $l = 0, 1, 2, \dots$ .] For typical systems the regime where  $\Omega$  is small compared to  $\omega_c$  occurs at experimentally available magnetic fields. The wavefunction for the orbital with angular momentum  $l$  is localised within  $\sim \ell$  of a circle of radius  $R_l$ , where  $R_l^2 \equiv \langle l|r^2|l \rangle = 2\ell^2(l+1)$ . (See Fig. 1.) The circle of radius  $R_l$  encloses magnetic flux  $(l+1)\Phi_0$ , where  $\Phi_0 = hc/e$  is the electron flux quantum. Orbitals at larger angular momentum are localised further from the minimum of the confinement potential and experience a stronger confinement potential. Note that in the lowest Landau level the single-particle orbitals all have the same sign of angular momentum. This consequence of broken time-reversal symmetry in the strong magnetic field limit leads to important simplifications. We will assume throughout this article that the magnetic field is strong enough that mixing of states in higher Landau levels by the electron-electron interaction can be neglected. We also assume that the electron system is completely spin-polarised by the magnetic field (for effects of spin degrees of freedom see Yang *et al.* 1993).

For non-interacting electrons the many-body ground state,  $|\Psi_0\rangle$ , is a single Slater determinant in which the confinement energy is minimised by occupying orbitals from  $l = 0$  to  $l = N - 1$ . This state is an exact many-body eigenstate of the Hamiltonian *even when electron-electron interactions are included*. The preceding claim follows after noting that the total angular momentum operator

$$\hat{L}_{tot} = \sum_{l=0}^{\infty} l\hat{n}_l \quad (1)$$

commutes with the Hamiltonian so that  $L_{tot}$  is a good quantum number, and that  $|\Psi_0\rangle$  is the only state in the Hilbert space with  $L_{tot} = N(N-1)/2$ . All other states have larger values of  $L_{tot}$ . However, once electron-electron interactions

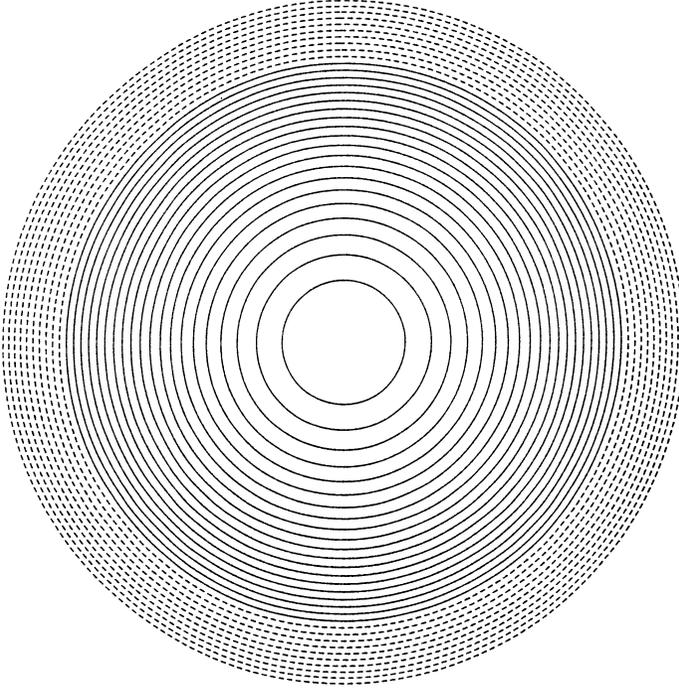


**Fig. 1.** Schematic representation of lowest Landau level orbits for a quantum dot in a magnetic field. With increasing radii, each circle encloses an additional unit of area and represents an orbital with an additional unit of angular momentum. Higher angular momentum orbitals are farther from the minimum of the confinement potential and have larger confinement energies. In an  $N$ -electron maximum-density-droplet (MDD) state the innermost  $N$  orbitals are occupied and others are empty. In this illustration the first twenty circles (solid lines) represent orbitals occupied in a twenty-electron MDD state, and the dashed circles represent unoccupied orbitals.

become important  $|\Psi_0\rangle$  need not be the ground state. In the lowest Landau level the total angular momentum operator can be written in the first-quantised form

$$\hat{L}_{tot} = \sum_i (r_i^2/2\ell^2 - 1). \quad (2)$$

If we assume that the electrons are confined to a droplet of roughly constant density, equation (2) may be used to relate  $L_{tot}$  to the average area of the droplet:

$$L_{tot} \sim NA/(4\pi\ell^2). \quad (3)$$

Many-body states with smaller area have smaller confinement energies, since the electrons are closer to the minimum of the confinement potential, but larger interaction energies, since the electrons are closer to each other. For sufficiently weak confinement the area of the ground state of an interacting-electron droplet will increase and  $|\Psi_0\rangle$  will no longer be the ground state.

The electron density in state  $|\Psi_0\rangle$  is

$$n(r) = \sum_{l=0}^{N-1} |\phi_l(z)|^2 = \frac{1}{2\pi\ell^2} \exp(-r^2/2\ell^2) \sum_{l=0}^{N-1} \frac{1}{l!} \left(\frac{r^2}{2\ell^2}\right)^l. \quad (4)$$

Except near the edges of the droplet,  $n(r) = (2\pi\ell^2)^{-1}$ . This is the maximum electron density that can be reached at any point without mixing states from higher Landau levels, and we therefore refer to  $|\Psi_0\rangle$  as the maximum density droplet (MDD) state. The energy of the MDD state is

$$E_{\text{MDD}} = \left(\frac{1}{2}\hbar\omega_c + \gamma\right)N + \gamma N(N+1)/2 + E_{\text{MDD}}^H + E_{\text{MDD}}^{\text{XC}}. \quad (5)$$

The first two terms on the right-hand side of equation (5) are the kinetic energy and confinement energies. The third term is the Hartree (electrostatic) energy, and the fourth term, the exchange-correlation energy, is defined by this equation. The Hartree energy of the MDD state is approximately equal to that of a disk with uniform areal number density  $\bar{n} = (2\pi\ell^2)^{-1}$ :

$$E_{\text{MDD}}^H \approx \frac{8e^2N^2}{3\pi\epsilon R_N} = \frac{e^2}{\epsilon\ell} \frac{4\sqrt{2}}{3\pi} N^{\frac{3}{2}}. \quad (6)$$

Here  $R_N = \sqrt{2N}\ell$  is the approximate radius of the  $N$ -electron MDD state. Corrections to this approximate expression for the Hartree energy and the exchange-correlation energy will both contribute terms  $\sim N$  to the MDD state energy.

One important property of dots which can be measured (see e.g. McEuen *et al.* 1991, 1992; Meir *et al.* 1991; Beenakker 1991) is the chemical potential change when a single electron is added to the system. If we define  $\mu(N)$  as the difference in energy between the  $(N+1)$ -electron ground state and the  $N$ -electron ground state, then for  $N \gg 1$  it follows from equations (5) and (6) that

$$\mu(N+1) - \mu(N) = \gamma + \frac{e^2}{\epsilon\ell} \frac{\sqrt{2}}{\pi} N^{-1/2} \quad (7)$$

up to terms vanishing as  $N^{-1}$ . For a system of particles with short-range interaction and confined to a fixed 'volume'  $\Omega \sim L^d$  in  $d$  dimensions,  $\mu(N+1) - \mu(N)$  vanishes as  $N^{-1}$ , leading to a chemical potential which depends only on particle density in the thermodynamic limit. For ordinary small metallic grains with  $e^2/\epsilon r$  interactions between the electrons this quantity vanishes, at fixed density, as  $N^{-1/d}$ ; the anomalously slow decrease of finite-size effects leads to the *Coulomb blockade* phenomena (see e.g. Zeller and Giaver 1969; Averin and Likharev 1991). We see from equation (7) that for parabolically confined two-dimensional systems in the strong magnetic field limit the term *Coulomb blockade* is something of a misnomer. The Coulomb energy scales in the same way as for metallic grains but the largest contribution to the chemical potential change comes in this case from the confinement energy. It may be difficult to separate these two contributions experimentally.

In the following sections we derive stability criteria for the MDD state. In Section 3 we consider the stability of the collective phonon-like edge excitations of the MDD. In the process we derive a useful exact identity relating Hartree–Fock self-energies and vertex functions of the quantum dot at the Fermi level. This identity is used to derive an exact expression for the chemical potential change on addition of a particle, which reduces to equation (7) in the large- $N$  limit. In Section 4 we consider the stability of the the MDD against the formation of a hole in the middle of the droplet. We find that, because of differences between two-dimensional and three-dimensional electrostatics, with weakening confinement the system becomes unstable to the introduction of holes in the bulk before the edge becomes unstable.

### 3. Stability of the MDD Edge

The total angular momentum of the MDD state,  $M_{\text{MDD}} = N(N-1)/2$ , is the smallest angular momentum in the Hilbert space. The low-energy excited states with total angular momentum  $M = M_{\text{MDD}} + \delta M$ , where  $\delta M \ll N$ , are states in which phonon-like (see e.g. Wen 1992; Stone 1990, 1991a, 1991b; Stone *et al.* 1992) collective modes have been excited at the edge of the MDD. In this section we discuss the conditions required for these edge excitation energies to be positive. If the edge excitation energies were not positive the MDD would not be the ground state. This is somewhat analogous to the soft phonon modes at wavevectors  $k_F$  and  $-k_F$  which combine to give charge-density-wave states. Here, however, edges are chiral ( $\delta M > 0$ ) so that if a state of nonzero  $\delta M$  became the ground state the system would retain its circular symmetry. In fact we present evidence that even this does not occur, that the instability of the ground state does not occur at the edge for parabolic quantum dots in a strong magnetic field.

The expectation value of the Hamiltonian in a single Slater determinant state (i.e. a state with definite occupation numbers  $n_m$  equal to 0 or 1) is

$$E[n_m] = \sum_m n_m \varepsilon_m + \frac{1}{2} \sum_{m,m'} n_m n_{m'} U_{m,m'}, \quad (8)$$

where

$$U_{m,m'} \equiv \langle m, m' | V | m, m' \rangle - \langle m', m | V | m, m' \rangle \quad (9)$$

is the difference of direct and exchange two-body matrix elements. Note that  $U_{m,m} = 0$ . We will show below that it is possible to express the excitation energies for  $\delta M = 1$  and  $\delta M = 2$  in terms of such expectation values, even though for  $\delta M = 2$  the eigenstates are not single Slater determinants. In the MDD state,  $n_m = 1$  for  $0 \leq m \leq N-1$  and is zero otherwise. Expanding the occupation numbers around the MDD-state values gives

$$E[n_m] = E_{\text{MDD}} + \sum_m \delta n_m \left( \varepsilon_m + \Sigma_m^{(N)} \right) + \frac{1}{2} \sum_{m,m'} \delta n_m \delta n_{m'} U_{m,m'}. \quad (10)$$

Here

$$\Sigma_m^{(N)} = \sum_{m'=0}^{N-1} U_{m,m'} \quad (11)$$

is the Hartree–Fock self-energy for the  $N$ -electron MDD state and  $\varepsilon_m + \Sigma_m^{(N)}$  is the Hartree–Fock quasiparticle energy. The Hartree–Fock self-energy is shown in Fig. 2 for an  $N = 40$  MDD state. We will see below that because of the broken time-reversal symmetry some properties of the system’s excitations are given exactly in terms of the Hartree–Fock self-energy.

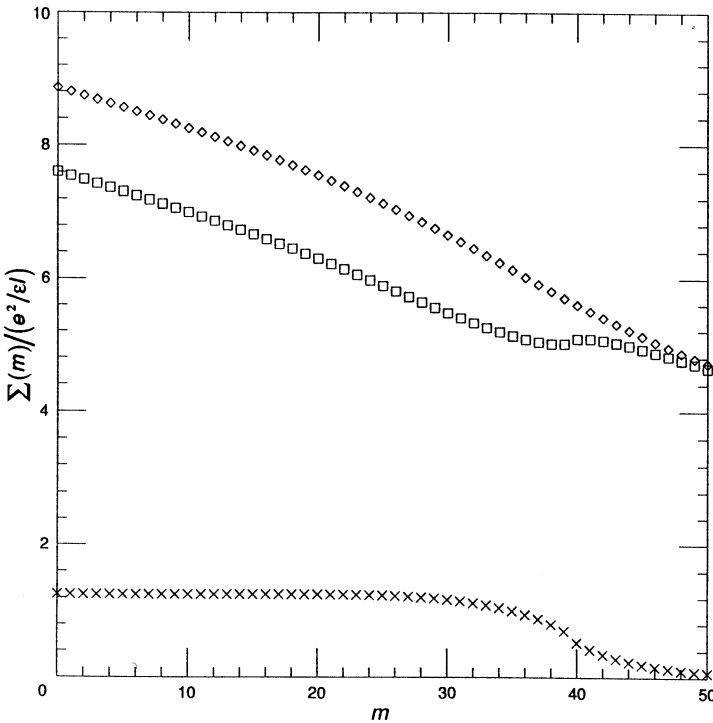


**Fig. 2.** Hartree–Fock self-energy [equation (11)] for  $m = 0$  to  $m = 50$  for the maximum-density droplet with  $N = 40$ . The diamonds show the Hartree self-energy, which neglects exchange, the squares show the full self-energy, and the crosses show the negative of the exchange energy.

We first consider the state with  $\delta M = 1$ . There is only one state in the Hilbert space at this angular momentum and it is therefore an exact eigenstate of the Hamiltonian. This state, which we label  $|1\rangle$ , has  $\delta n_N = 1$  and  $\delta n_{N-1} = -1$ , as illustrated in Fig. 3. From equation (10) it follows that

$$E_1 = E_{\text{MDD}} + \gamma + \Sigma_N^{(N)} - \Sigma_{N-1}^{(N)} - U_{N,N-1}. \quad (12)$$

(In a perturbative treatment the contribution  $U_{N,N-1}$  to the excitation energy would appear through vertex corrections to a two-particle Green’s function.)

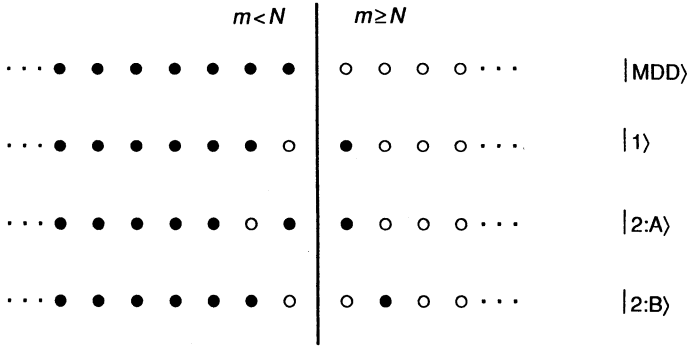


**Fig. 3.** Occupation numbers for the states considered in this section. Occupied states are indicated by solid circles and unoccupied states by open circles.

However,  $|1\rangle$  differs from the MDD state only through an excitation of the centre of mass. To see this it is convenient to define a first-quantised ladder operator for centre-of-mass (COM) states in the lowest Landau level:

$$B^\dagger = \frac{1}{\sqrt{N}} \sum_i b_i^\dagger. \tag{13}$$

Here  $b_i^\dagger = (z_i/2\ell - 2\ell\partial/\partial\bar{z}_i)/\sqrt{2}$  is the intra-Landau-level single-particle ladder operator (see e.g. MacDonald 1991) which can be used to generate the angular momentum eigenstates in the Landau gauge ( $b^\dagger|m\rangle = \sqrt{m+1}|m+1\rangle$ ). The COM states in the lowest Landau level have the same set of angular momenta as the single-particle states and are generated from the zero angular momentum COM state by  $B^\dagger$ . In second-quantised form  $B^\dagger$  and the COM angular momentum operator  $\hat{M}_{\text{COM}} = B^\dagger B$  can be written

$$\hat{B}^\dagger = \frac{1}{\sqrt{N}} \sum_m \sqrt{m+1} \hat{c}_{m+1}^\dagger \hat{c}_m, \tag{14}$$

$$\hat{M}_{\text{COM}} = \frac{1}{N} \left[ \sum_{m>0} \hat{n}_m m + \sum_{m,m'} \sqrt{(m+1)m'} \hat{c}_{m+1}^\dagger \hat{c}_{m'-1}^\dagger \hat{c}_{m'} \hat{c}_m \right]. \tag{15}$$

Here  $\hat{c}_m^\dagger$  creates an electron in the single-particle state  $\phi_m$  in the lowest Landau level. The  $\hat{B}$  and  $\hat{B}^\dagger$  obey boson commutation relations:  $[\hat{B}, \hat{B}^\dagger] = \sum_m \hat{n}_m/N$ , which is unity in the  $N$ -electron sector. It is easy to verify that  $|MDD\rangle$  is an eigenstate of  $\hat{M}_{\text{COM}}$  with eigenvalue zero, and that  $B^\dagger|MDD\rangle = |1\rangle$ . Since  $B^\dagger$  operates only on the COM degree of freedom, it commutes with the interaction part of the Hamiltonian (see e.g. Trugman and Kivelson 1985) and

$$[H, B^\dagger] = \gamma B^\dagger. \tag{16}$$

It follows that  $E_1 = E_{\text{MDD}} + \gamma$ . Note that  $|1\rangle$  has a higher energy than  $|MDD\rangle$  no matter how weak the confinement. Comparing with equation (12) it follows that

$$\Sigma_N^{(N)} = \Sigma_{N-1}^{(N)} + U_{N,N-1}. \quad (17)$$

This exact relationship between the self-energy and the vertex correction is a consequence of the fact that the relative motions in  $|MDD\rangle$  and  $|1\rangle$  are identical. We will use this relationship below to calculate the energies of the  $\delta M = 2$  states.

This approach to generating edge excitations has been used for other purposes. In first-quantised language, a bosonic basis for the edge excitations can be constructed by the power sums (see e.g. Stone 1990, 1991*a*, 1991*b*; Stone *et al.* 1992)  $S_k = \sum_i z_i^k$ . The  $M = M_{\text{MDD}} + \delta M$  subspace is spanned by the set of products  $\{S_1^{l_1} S_2^{l_2} S_3^{l_3} \dots\} |MDD\rangle$  with  $\sum_k k l_k = \delta M$ . The operator  $B^\dagger$  given in equation (13) is, when acting on states in the lowest Landau level, equivalent to  $S_1$  times a normalisation constant. ( $B^\dagger$  is written in terms of  $b_i^\dagger$ , while  $S_1$  is written in terms of  $z_i$ —the benefit of the former is that its adjoint is easy to determine.) The operator  $\hat{B}^\dagger$  is thus the second-quantised form of  $S_1$ , and second-quantised versions of the remaining  $S_k$  have also been constructed (Marsili 1993): to within a normalisation constant,  $\hat{B}_k^\dagger = \sum_m \sqrt{(m+k)!/m!} \hat{c}_{m+k}^\dagger \hat{c}_m$ . Only for  $k = 1$  (the case discussed above) does the operator  $\hat{B}_k^\dagger$  generate an eigenstate for finite  $N$ .

There are two states in the many-body Hilbert space with  $\delta M = 2$ ; one has  $\delta n_{N-2} = -1$  and  $\delta n_N = 1$  and is labeled as state  $|2:A\rangle$  in Fig. 3, while the other has  $\delta n_{N-1} = -1$  and  $\delta n_{N+1} = 1$  and is labeled  $|2:B\rangle$  in Fig. 3. We can easily generate one of the two eigenstates at  $\delta M = 2$  by using the COM angular-momentum raising operator

$$|2; +\rangle \equiv \frac{1}{\sqrt{2}} (B^\dagger)^2 |MDD\rangle. \quad (18)$$

It follows from equation (16) that  $|2; +\rangle$  is an eigenstate of the Hamiltonian with eigenvalue  $E_{2+} = E_{\text{MDD}} + 2\gamma$ . Applying  $\hat{B}^\dagger$  twice, we see that

$$|2; +\rangle = \left(\frac{N-1}{2N}\right)^{\frac{1}{2}} |A\rangle + \left(\frac{N+1}{2N}\right)^{\frac{1}{2}} |B\rangle. \quad (19)$$

The other eigenstate at  $\delta M = 2$  must be orthogonal to this, so

$$|2; -\rangle = \left(\frac{N+1}{2N}\right)^{\frac{1}{2}} |A\rangle - \left(\frac{N-1}{2N}\right)^{\frac{1}{2}} |B\rangle. \quad (20)$$

(This state can be written as a linear combination  $[\alpha \hat{B}_2^\dagger + \beta (\hat{B}^\dagger)^2] |MDD\rangle$ . In the limit  $N \rightarrow \infty$ ,  $\beta$  approaches zero.)

It follows that the eigenenergy of this state is  $E_{2-} = E_{\text{MDD}} + 2\gamma + \delta E$ , where

$$\delta E = 2N[(\langle A|\hat{V}|A\rangle - E_{\text{MDD}}^{\text{int}})/(N+1) - 2N[(\langle B|\hat{V}|B\rangle - E_{\text{MDD}}^{\text{int}})/(N-1)]. \quad (21)$$

(Here  $E_{\text{MDD}}^{\text{int}} = E_{\text{MDD}}^H + E_{\text{MDD}}^{XC}$  is the interaction energy in the MDD state.) This can be shown in two steps. First, calculate the expected energies of  $|2; +\rangle$  and  $|2; -\rangle$  and use the known value of the former to eliminate the off-diagonal matrix element  $\langle A|\hat{V}|B\rangle$ . Second, solve the  $2 \times 2$  Hamiltonian with basis states  $|A\rangle$  and  $|B\rangle$ , and require that the resulting eigenstates be equations (19) and (20); this gives equation (21). From equations (10), (11) and (17) it then follows that

$$\langle A|\hat{V}|A\rangle = E_{\text{MDD}}^{\text{int}} + U_{N,N-1} - U_{N+1,N-1}. \quad (22)$$

We have thus succeeded in expressing the eigenenergies for  $\delta M = 2$  in terms of interaction matrix elements near the edge of the dot.

For large  $N$  the above results may be used to obtain a necessary condition for the stability of the maximum density droplet. As illustrated in Fig. 1 the single-particle orbital with angular momentum  $N$  is localised within about  $\ell$  of a circle of radius  $R_N = \sqrt{2N}\ell$ . If we ignore the width of the resulting annulus in comparison with its circumference, an approximation which becomes increasingly accurate as  $N$  increases, we obtain, for  $M \sim N$ ,

$$U_{N,M} \approx \frac{e^2}{4\pi\epsilon R_N} \int_0^{2\pi} \frac{1 - \cos[(N-M)\theta]}{\sin(\theta/2)} d\theta = \frac{2e^2}{\epsilon R_N \pi} \sum_{l=1}^{|N-M|} \frac{1}{2l-1}. \quad (23)$$

The second term in the numerator of the integrand for the integral over  $\theta$  comes from the exchange term. If this term were not present  $U_{N,N\pm k}$  ( $k \ll N$ ) would be logarithmically larger for large  $N$ :  $U_{N,N\pm k} \sim (e^2 \ln(R_N/\ell))/(2\epsilon R_N)$ . Comparing equations (23), (22) and (21), we see that for large  $N$

$$E_{2-} - E_{\text{MDD}} = 2\gamma - \frac{4e^2}{3\pi\epsilon R_N}. \quad (24)$$

The interaction energy is lowered in this state because the electrons are spread over a slightly larger area. In  $|2; +\rangle$ , on the other hand, the COM of the droplet is not as well localised but the area of the droplet stays the same. We can conclude from the above exact result that the MDD state becomes unstable at the edge if

$$\frac{\gamma}{e^2/\epsilon\ell} < \frac{\sqrt{2}}{3\pi N^{1/2}} = 0.15005N^{-1/2}. \quad (25)$$

We should now consider the possibility that the edge instability occurs first for larger  $\delta M$ . For  $\delta M = 3$  there are three states, two of which we can easily generate using the COM angular momentum raising operator:  $B^\dagger|2, +\rangle/\sqrt{3}$  and  $B^\dagger|2, -\rangle$ . These two states have energies larger by  $\gamma$  than  $|2; +\rangle$  and  $|2; -\rangle$ , respectively, and are always more stable than states already considered. The third eigenstate is the one orthogonal to these two, and its energy could be evaluated using the same approach as above. It has all of its excess angular momentum

in the relative motion of the electrons and should be the lowest energy  $\delta M = 3$  state. Although we have not yet completed this calculation we expect that the third state becomes unstable before  $|2; -\rangle$ . However, as we show in the following section, it becomes energetically favourable to introduce holes in the bulk of the MDD well before the edge of the MDD becomes unstable. The first instability occurs at  $\delta M \simeq N$  for an  $N$ -electron droplet and does not correspond to an edge excitation.

The results in this section can be used to derive a simple exact expression for the chemical potential change on addition of a particle. Defining  $\mu(N)$  as the difference in energy between the  $(N+1)$ -electron ground state and the  $N$ -electron ground state, as earlier, it follows from equation (10) that  $\mu(N) = \gamma N + \Sigma_N^{(N)}$ . Using equations (11) and (17) it then follows that

$$\mu(N+1) - \mu(N) = \gamma + U_{N+1,N}. \quad (26)$$

Using equation (23) for  $U_{N+1,N}$  at large  $N$  we recover the results of equation (7). We emphasise that even though these results are expressed in terms of Hartree–Fock approximations they are in fact exact as long as the MDD state remains the ground state.

#### 4. Bulk Hole Instability

In this section we consider the single Slater determinant  $|1H\rangle$ , which differs from the maximum density droplet by having  $\delta n_0 = -1$  and  $\delta n_N = 1$ . This state differs from the states  $|1\rangle$  and  $|2:A\rangle$  only in that the orbital that is emptied is at the centre of the droplet. The state can be considered as an  $(N+1)$ -electron droplet with a hole at the centre. Unlike the cases discussed above there are many  $N$ -particle states of the droplet with the same total angular momentum as  $|1H\rangle$ . However the coupling between  $|1H\rangle$  and the other states is weak for large droplets and we will ignore it in the discussion below. (The states with the same angular momentum as  $|1H\rangle$  have the hole in a state of angular momentum  $m$  and the edge of the  $(N+1)$ -electron droplet in a state with the same excess angular momentum. The coupling matrix elements can be shown to scale as  $e^2 \ell^m / \varepsilon R_N^{m+1}$ .) Using equation (10) we see that the energy of the hole state is

$$E_{1H} = E_{\text{MDD}} + N\gamma + \Sigma_N^{(N)} - \Sigma_0^{(N)} - U_{0,N}. \quad (27)$$

The last term represents an excitonic attraction between the hole and the extra charge at the edge, is proportional to  $N^{-1/2}$ , and becomes negligible for large dots. The Hartree contribution to the self-energies can be estimated from the Hartree potential of a uniformly charged droplet of radius  $R_N$ , as discussed in Section 2:

$$V_H^{(N)}(r) = \frac{2Ne^2}{\varepsilon R_N} F\left(\frac{1}{2}, -\frac{1}{2}; 1, \frac{r^2}{R^2}\right), \quad (28)$$

which is plotted in Fig. 4. Note that this potential decreases more rapidly with distance from the centre than the analogous potential for a uniformly charged sphere. The different behaviour can be related to the larger fraction of

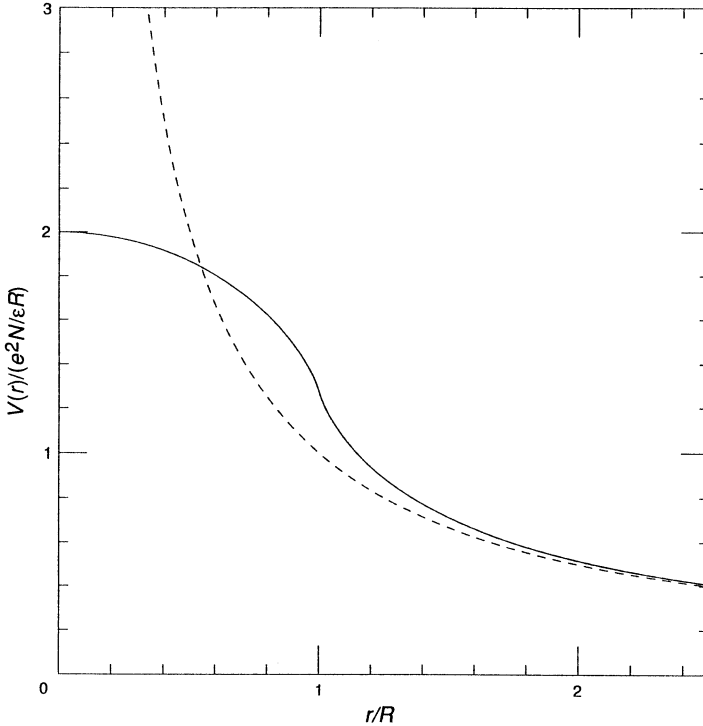


**Fig. 4.** Hartree potential from a uniformly charged disk of radius  $R$ . Unlike the three-dimensional case the potential is larger at the centre of the disk than at the edge. The dashed curve shows the potential when the charge is collapsed to a point at the centre of the disk.

charge inside a given radius in the two-dimensional case. This difference between two-dimensional and three-dimensional electrostatics plays a very important role in determining the properties of quantum dots, particularly in the strong magnetic field limit as we see below.

Note that the Hartree potential is proportional to  $N^{\frac{1}{2}}$ , so that for large droplets the exchange contribution to the self-energy is negligible by comparison. Taking  $\Sigma_N^{(N)} - \Sigma_0^{(N)} \approx V_H^{(N)}(R_N) - V_H^{(N)}(0) = (Ne^2/\epsilon R_N)(4/\pi - 2)$ , we see that for large dots it becomes favourable to introduce holes at the centre of the MDD state whenever

$$\frac{\gamma}{e^2/\epsilon\ell} < \frac{\sqrt{2} - \sqrt{8}/\pi}{N^{\frac{1}{2}}} = 0.51390N^{-1/2}. \tag{29}$$

Expanding equation (28) near the centre of the droplet, we see that the sum of confinement and Hartree potentials is given by

$$V_{\text{CH}}(r) = \frac{e^2\sqrt{2N}}{\epsilon\ell} + \left(\frac{r^2}{R_N}\right)^2 [\gamma N - N^{\frac{1}{2}}(e^2/\epsilon\ell)/\sqrt{8}]. \tag{30}$$

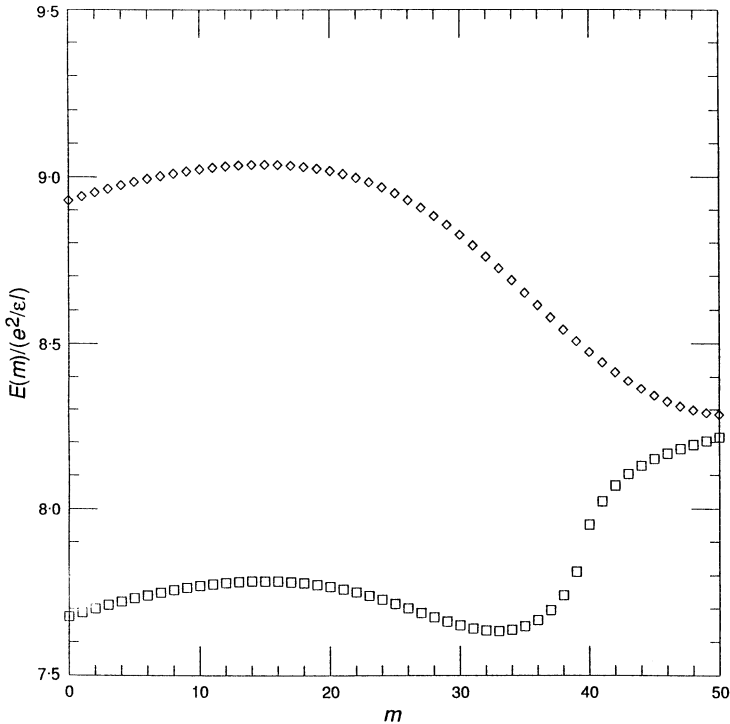


**Fig. 5.** Hartree-Fock quasiparticle energies for  $m = 0$  to  $m = 50$  (squares), for  $N = 40$  and  $\gamma = 0.07e^2/\epsilon\ell$ . Note that the occupied orbitals all have lower energies than any unoccupied orbital. The proximity of the bulk hole instability is evident. The diamonds show the quasiparticle energies in the Hartree approximation where exchange is neglected.

At the point where it becomes favourable to introduce holes at the centre of the droplet, the quasiparticle energy will increase with angular momentum. It follows that holes will be introduced first in the bulk, away from the centre of the droplet and at a slightly larger value of  $\gamma$  than that required for the introduction of holes at the centre of the droplet. Detailed results, given elsewhere (see e.g. Yang *et al.* 1993), depend on the number of electrons in the droplet and require numerical calculations.

The introduction of holes in the bulk of the dot pre-empts the edge instability discussed in the previous section. The holes in the bulk of the droplet increase the strength of the confinement field seen at the edge of the disk and prevent the edge from becoming unstable as the density is lowered further. In Fig. 5 we plot the Hartree-Fock quasiparticle energies for an  $N = 40$  MDD state including a single-particle contribution for  $\gamma = 0.07(e^2/\epsilon\ell)$ . This value is just large enough to ensure stability and may be compared with the critical  $\gamma$  for holes at the centre of the droplet obtained from the above large- $N$  approximation which gives  $\gamma \sim 0.08(e^2/\epsilon\ell)$ . Note that for a droplet of this size the instability will occur first for  $m \sim 15$ , corresponding to  $\delta M \sim 25$ . Also plotted in Fig. 5 are the quasiparticle energies obtained neglecting the exchange contribution. We see

that the MDD state is already unstable if exchange is neglected. The Hartree approximation seriously underestimates the stability of the MDD state and would lead to qualitatively incorrect results.

## 5. Summary and Concluding Remarks

For non-interacting electrons the ground state of a parabolically confined  $N$ -electron quantum dot at strong magnetic fields has the single-particle orbitals with  $m = 0, 1, \dots, N - 2, N - 1$  occupied. Because of the strongly broken time-reversal symmetry at strong magnetic fields, this maximum-density-droplet state remains an exact eigenstate of the Hamiltonian including electron-electron interactions. In this paper we have examined the conditions required for the MDD to remain the ground state. We have found that for large dots the MDD is unstable toward edge excitations for  $\gamma/(e^2/\epsilon\ell) < 0.15005N^{-1/2}$ , where  $\gamma$  is a parameter that measures the strength of the confinement potential. However, for  $\gamma/(e^2/\epsilon\ell) < 0.51390N^{-1/2}$  we find that the MDD is unstable toward the introduction of holes at the centre of the system. This behaviour is directly related to differences between two-dimensional and three-dimensional electrostatics. The critical value of  $\gamma$  at which holes are introduced in the lowest Landau level will, at least for large droplets, be approximately equal to the value of  $\gamma$  at which the spins first become fully spin-polarised (see e.g. Yang *et al.* 1993). These small values of  $\gamma$  are those at which the fractional Hall regime is first being approached in quantum dots. For quantum dots in GaAs,  $\gamma \sim 0.58(\hbar\Omega[\text{meV}])^2/B[\text{Tesla}]$ . Thus it seems that this regime can be reached with magnetic fields available in the laboratory.

## Acknowledgments

One of us (AHM) acknowledges the hospitality and support of the School of Physics at the University of New South Wales during the period when this article sprang to life. This work was supported in part by the National Science Foundation under grant DMR-9113911 and in part by the UCF Division of Sponsored Research.

## References

- Averin, D. V., and Likharev, K. K. (1991). In 'Mesoscopic Phenomena in Solids' (Eds B. L. Altschuler, P. A. Lee, and R. A. Webb) (Elsevier: Amsterdam).
- Beenakker, C. W. J. (1991). *Phys. Rev. B* **44**, 1646.
- Chakraborty, T. (1992). *Comments Condensed Matter Phys.* **16**, 35.
- Hansen, W., Smith, T. P. III, Lee, K. Y., Brum, J. A., Knoedler, C. M., Hong, J. M., and Kern, D. P. (1989). *Phys. Rev. Lett.* **62**, 2168.
- Kastner, M. A. (1992). *Rev. Mod. Phys.* **64**, 849.
- von Klitzing, K., Dorda, G., and Pepper, M. (1980). *Phys. Rev. Lett.* **45**, 494.
- MacDonald, A. H. (1991). In 'Quantum Coherence in Mesoscopic Systems' (Ed. B. Kramer) (Plenum: New York).
- MacDonald, A. H., and Johnson, M. D. (1993). *Phys. Rev. Lett.* **70**, 3107.
- McEuen, P. L., Foxman, E. B., Kinaret, J., Meirav, U., Kastner, M. A., Wingreen, N. S., and Wind, S. J. (1992). *Phys. Rev. B* **45**, 11419.
- McEuen, P. L., Foxman, E. B., Meirav, U., Kastner, M. A., Meir, Y., Wingreen, N. S., and Wind, S. J. (1991). *Phys. Rev. Lett.* **66**, 1926.
- Marsili, M. (1993). *Phys. Rev. B* (submitted for publication).
- Meir, Y., Wingreen, N. S., and Lee, P. A. (1991). *Phys. Rev. Lett.* **66**, 3048.

- Merkt, U. (1990). *Adv. Solid State Phys.* **30**, 77.
- Stone, M. (1990). *Phys. Rev. B* **42**, 8299.
- Stone, M. (1991). *Ann. Phys. (NY)* **207**, 38.
- Stone, M. (1991). *Int. J. Mod. Phys. B* **5**, 509.
- Stone, M., Wyld, H. W., and Schult, R. L. (1992). *Phys. Rev. B* **45**, 14156.
- Trugman, S. A., and Kivelson, S. (1985). *Phys. Rev. B* **31**, 5280.
- Tsui, D. C., Stormer, H. L., and Gossard, A. C. (1982). *Phys. Rev. Lett.* **48**, 1559.
- Wen, X. G. (1992). *Int. J. Mod. Phys. B* **6**, 1711.
- Yang, S.-R. E., MacDonald, A. H., and Johnson, M. D. (1993). *Phys. Rev. B* (submitted for publication).
- Zeller, H. R., and Giaver, I. (1969). *Phys. Rev.* **181**, 789.

Manuscript received 18 December 1992, accepted 7 April 1993